Energy Engineering

Tech Science Press

DOI: 10.32604/ee.2023.027790

ARTICLE

An Investigation of Battery Energy Storage Aided Wind-Coal Integrated Energy System

Enhui Sun[1,2], Jiahao Shi[1,2], Lei Zhang[1,2,*], Hongfu Ji[1,2], Qian Zhang[1,2] and Yongyi Li[1,2]

[1]Department of Power Engineering, North China Electric Power University, Baoding, 071003, China

[2]Hebei Key Laboratory of Low Carbon and High Efficiency Power Generation Technology, Baoding, 071003, China

[*]Corresponding Author: Lei Zhang. Email: zhang_lei@ncepu.edu.cn

Received: 15 November 2022 Accepted: 30 January 2023 Published: 01 May 2023

ABSTRACT

This paper studies the feasibility of a supply-side wind-coal integrated energy system. Based on grid-side data, the load regulation model of coal-fired power and the wind-coal integrated energy system model are established. According to the simulation results, the reasons why the wind-coal combined power supply is difficult to meet the grid-side demand are revealed through scenario analysis. Based on the wind-coal combined operation, a wind-coal-storage integrated energy system was proposed by adding lithium-iron phosphate battery energy storage system (LIPBESS) to adjust the load of the system. According to the four load adjustment scenarios of grid-side instructions of the wind-coal system, the difficulty of load adjustment in each scenario is analyzed. Based on the priority degree of LIPBESS charge/discharge in four scenarios at different time periods, the operation mode of two charges and two discharges per day was developed. Based on the independent operation level of coal-fired power, after the addition of LIPBESS (5.5 MWh), the average qualified rate of multi-power operation in March and June reached the level of independent operation of coal-fired power, while the average qualified rate of the remaining months was only 5.4% different from that of independent operation of coal-fired power. Compared with the wind storage mode, the energy storage capacity and investment cost of wind-coal-storage integrated energy system are reduced by 54.2% and 53.7%, respectively.

KEYWORDS

Wind power; lithium-iron phosphate battery energy storage system; coal-fired power; integrated energy system

1 Introduction

The random and fluctuating characteristics of wind power affect the safety and economy of the power grid [1]. The anti-peak regulation of wind power generation results in serious wind power abandoning phenomenon [2]. These problems could hamper the development of wind power and need to be solved to increase the proportion of wind power in the grid [3].

The combination of energy storage system and wind power is considered as an effective way to improve the stability of wind power: (1) Thermal energy storage [4]. (2) Hydropower and pumped storage [5]. (3) Compressed air energy storage [6]. (4) Battery energy storage system (BESS) [7]. BESS is a relatively mature energy storage technology, which has the superiorities of fast response, stability, and geographical independence and it has been triumphantly applied to various application scenarios [8]. It is an ideal auxiliary adjustment method for the power system, but the economy is the main problem

restricting its application [9]. Thus, flexible power generation systems are needed to co-dispatch wind power to reduce battery energy storage capacity.

Wind power can be effectively utilized by dispatching through hydropower [10]. However, the geographical distribution of hydropower is limited, so relying on them alone cannot significantly increase the proportion of wind power into the grid. Compared with hydropower, coal-fired power plants are not constrained by geography and have power regulation flexibility, which is a favorable choice for the integrated energy system of multi-source power [11]. Meantime, its operation technology is relatively mature, the highest ramp rate can reach 3%–4.5%, the minimum load is 25%–40% of rated capacity [12]. In the power system dominated by renewable energy, higher requirements are put forward for the flexibility of coal-fired power plants [13,14]. Frew et al. pointed out that coal-fired power plants with higher ramp rate and low load operation are more suitable for the power system with high renewable energy ratio [15]. Research shows that future power systems will require more flexibility from coal-fired power to increase the proportion of wind power [16].

The wind-coal integrated energy system has been investigated by some researchers. Li et al. proposed that power generation planning for thermal power, wind power and solar power would help enhance the economic benefits [17]. Gao et al.'s research showed that thermal power and wind power can promote the utilization of wind power and increase the flexibility of power system through reasonable planning [18]. Dong et al. showed that the wind-coal combined dispatching can reduce pollution emission by optimizing operation strategy [19]. Zhu et al. studied the impact of the system costs and emissions with different wind and thermal capacity combinations [20]. Dong et al. solved the problem of unstable power supply from wind power by adding energy storage system, thus reducing the influence of wind power on coal-fired power [21]. The above research mainly focuses on the economics and low carbon emissions of power dispatching. However, coal-fired power has the potential to dispatch wind power as a flexible power system. In addition, the BESS has higher charge and discharge power, which can incorporation with the coal-fired power and enhance the flexibility of multi-source power integrated energy system. At present, there is insufficient research to show the feasibility of dispatching wind power directly through the coal-fired power, it is necessary to further explore the potential of direct dispatching of wind power from coal-fired power. Therefore, different from previous studies, this paper explores the feasibility of coal power directly acting as a regulatory power source to regulate wind power and respond to grid side command demands from the perspective of power matching.

In this paper, a wind-coal-storage integrated energy system operation mode is proposed, in which the battery energy storage system assists the coal-fired power generation to regulate the wind power generation. Explore the potential of dispatching wind power in coal-fired power to solve the problem of insufficient utilization of wind power. The research carried out in this paper is as follows: (1) The load model of coal-fired power plant based on historical operation data and battery energy storage system model are established, and the mathematical description and solution method are provided. (2) Through scenario analysis, the reasons for the efficiency reduction of the wind-coal integrated energy system are revealed, and the operation strategy of the energy storage system is formulated according to the load adjustment difficulty of each scenario. (3) Energy storage capacity is optimized through particle swarm optimization algorithm (PSO) based on the wind-coal-storage integrated energy system to reduce the investment of BESS.

2 Methodology

The frequency and power of the grid are primarily regulated by automatic generation control (AGC). Power plants respond to AGC instructions by adjusting the load to incorporate electricity into the power grid, which would be supplied to the user side after dispatching. Fig. 1a shows the operation mode of existing power plants responding to the AGC of the grid. However, wind power has the problem of power curtailment due to its natural characteristics. In the most severe areas, the wind power abandonment rate can reach 20% due to its volatility characteristics [22]. The wind-coal integrated energy system is shown in Fig. 1b, which utilizes the flexibility of coal-fired power to regulate wind power and supply electricity to the power grid. The research is based on 6-month historical data of a 50 MW wind farm and a 330 MW coal-fired power plant, and the main parameters of coal electricity are shown in Table 1 [23].

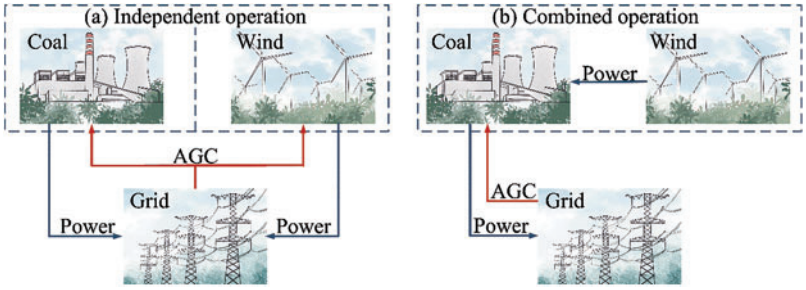

Figure 1: Power dispatching diagram of wind power, coal-fired power, and wind-coal combined operation

Table 1: Main parameters of coal-fired power

Parameter	Unit	BMCR
Main steam flow	t/h	1102
Main steam outlet pressure	MPa	17.5
Main steam outlet temperature	°C	541
Superheated vapor pressure drop	MPa	1.5
Feed water pressure	MPa	19.392
Feed water temperature	°C	280
Reheat steam flow rate	t/h	909.7
Reheat steam outlet pressure	MPa	3.617
Reheat steam outlet temperature	°C	541
Reheat steam inlet pressure	MPa	3.797
Reheat steam inlet temperature	°C	329.9

2.1 Mathematical Description

2.1.1 The Load Model of Coal-Fired Power Plant

The coal-fired power is a complex power generation system that involves a lot of heat transfer, mass transfer, and phase change processes. Thus, the load response has an inertial delay. The existing control methods of power plants are mainly based on automatic control to realize the coordination control of various systems. The automatic control of coal-fired power is mostly rely on the Proportional, Integral,

and Derivative (PID) controller for power regulation. Therefore, a load response model of a coal-fired power based on the PID control principle is built to simulate the load response process of the actual plant.

The mathematical description of the coal-fired power model is as follows:

$$(\Delta P)_{ij} = k_1\left[\left(P_{\mathrm{AGC,C}}\right)_{ij} - (P_{\mathrm{C}})_{(i-1)j}\right] + k_2\frac{1}{T_1}\int_{t_{1j}}^{t_{ij}}\left[\left(P_{\mathrm{AGC,C}}\right)_{ij} - (P_{\mathrm{C}})_{(i-1)j}\right]dt + k_3\frac{1}{T_2}\frac{d\left[\left(P_{\mathrm{AGC,C}}\right)_{ij} - (P_{\mathrm{C}})_{(i-1)j}\right]}{dt} \tag{1}$$

$$(P_{\mathrm{C}})_{ij} = (P_{\mathrm{C}})_{(i-1)j} + (\Delta P)_{ij}\,,\ \Delta P \le v_{\mathrm{r,max}} \tag{2}$$

where, i is the daily corresponding time, j is the running date ($i = 1,2,3,\ldots, 86400$; $j = 1, 2, 3\ldots$); $(P_{\mathrm{AGC,C}})_{ij}$ is the load command issued by the power grid at a certain time on the same day; P_{C} is the real-time load of coal-fired power; ΔP refers to the load adjustment value of the coal-fired power at the next time on the day; k_1, k_2, k_3 are the control coefficients of the coal power load regulation model, respectively, which need to be solved by actual data fitting; $v_{\mathrm{r,\,max}}$ refers to the daily stable climbing rate of coal-fired power.

2.1.2 The Principle of the Wind-Coal Integrated Energy System

In the combined wind-coal integrated energy system mode, coal-fired power is used as a regulatory power source to regulate wind power and respond to grid instructions, giving full play to the load regulation potential of coal-fired power and realizing stable power supply. The mathematical description of grid side instruction construction of wind-coal combined power supply system is as follows:

$$P_{\mathrm{AGC}}^{\mathrm{W\&C}}\begin{bmatrix} P_{1,1} & \cdots & P_{1,j} \\ \vdots & \ddots & \vdots \\ P_{i,1} & \cdots & P_{i,j} \end{bmatrix} = P_{\mathrm{AGC,C}}\begin{bmatrix} P_{1,1} & \cdots & P_{1,j} \\ \vdots & \ddots & \vdots \\ P_{i,1} & \cdots & P_{i,j} \end{bmatrix} + P_{\mathrm{AGC,W}}\begin{bmatrix} P_{1,1} & \cdots & P_{1,j} \\ \vdots & \ddots & \vdots \\ P_{i,1} & \cdots & P_{i,j} \end{bmatrix} \tag{3}$$

where, $P_{\mathrm{AGC}}^{\mathrm{W\&C}}$ is wind-coal combined power supply system AGC instructions; $P_{\mathrm{AGC,C}}$ is coal-fired power data AGC instruction; $P_{\mathrm{AGC,W}}$ is the original AGC instructions for wind power.

$$P_{\mathrm{ct}}^{\mathrm{W\&C}}\begin{bmatrix} P_{1,1} & \cdots & P_{1,j} \\ \vdots & \ddots & \vdots \\ P_{i,1} & \cdots & P_{i,j} \end{bmatrix} = P_{\mathrm{AGC}}^{\mathrm{W\&C}}\begin{bmatrix} P_{1,1} & \cdots & P_{1,j} \\ \vdots & \ddots & \vdots \\ P_{i,1} & \cdots & P_{i,j} \end{bmatrix} - P_{\mathrm{W}}\begin{bmatrix} P_{1,1} & \cdots & P_{1,j} \\ \vdots & \ddots & \vdots \\ P_{i,1} & \cdots & P_{i,j} \end{bmatrix} \tag{4}$$

where, $P_{\mathrm{ct}}^{\mathrm{W\&C}}$ is the power supply target of coal-fired power in the wind-coal combined power supply system. P_{W} indicates the wind power generation power. The load command of the combined power supply system is obtained by coupling the wind power plant with the coal power supply command. When wind power and coal power are coupled, short AGC deviation data segments will appear. AGC usually lasts at least 30 s. If the length of the coupled data segment is less than 30 s, it will be suppressed by the previous AGC instruction value. The coal-fired electricity simulation is calculated by the coupled AGC into the load regulation model, and the wind power load is linearly interpolated into second level data through actual minute level data.

2.1.3 Lithium-Iron Phosphate Battery Energy Storage System in Wind-Coal-Storage Integrated Energy System

Lithium-iron phosphate batteries are valued in battery energy storage systems for their advantages of lightweight, high energy conversion efficiency (85%–95%), and long cycle times (2000–10000 times) [24]. The lithium-iron phosphate battery energy storage system (LIPBESS) is composed of battery cells in series or parallel, each of them is constrained by the battery management system (BMS). It has security, monitoring, communication, control, and other functions. The direct-current output of the battery is connected to a power conversion system (PCS), which converts the power between alternating-current and direct-current output [25]. LIPBESS achieves target power charge and discharges under the management of BMS and PCS, the high charge and discharge speed and efficiency enable LIPBESS to start up quickly in energy storage system applications, providing technical support for rapid charge and discharge mode conversion of energy storage systems [26]. Thus, the energy storage system in this paper is based on LIPBESS. However, frequent charging and discharging will shorten its service life. The purpose of adding LIPBESS in this paper is to assist the system in improving the power regulation ability of integrated energy system. On the other hand, reducing the operating frequency of BESS might help increase its service life.

In this paper, the charge-discharge characteristics of LIPBESS were studied. The influences of cycle life, operation and maintenance, and operation faults on the use of LIPBESS were not considered in the construction of the model. The model constraints are as follows:

$$\eta_{\mathrm{BESS}} = 0.9 \tag{5}$$

where, η_{BESS} is the energy conversion efficiency of BESS, determine this parameter from the literature [26].

The State of Charge (SOC) of a battery is a state parameter that represents the battery capacity. SOC is calculated as follows:

$$\mathrm{SOC}_{t_2 j} = \mathrm{SOC}_{t_1 j} + \frac{1}{\mathrm{B}} \int_{t_1}^{t_2} \lambda P_{tj} \mathrm{d}t \tag{6}$$

$$10\% \leq \mathrm{SOC} \leq 90\% \tag{7}$$

where, P_{tj} is the charging or discharging power of the battery energy storage system at a certain time on the same day. SOC_{t1} is the initial SOC value of LIPBESS running, The SOC constraints of the model were obtained from the literature parameters [8,27]. B is the rated capacity of LIPBESS; t_1 is the initial time of LIPBESS operation; t_2 is the end time of LIPBESS operation; λ is a constant coefficient considering environmental factors such as temperature and aging. Eq. (7) is the SOC limit of LIPBESS. Meanwhile, in order to prevent LIPBESS from over-charging and over-discharge and ensure the safe and stable operation of the system, the SOC of LIPBESS is constrained.

During operation, LIPBESS improves the load regulation capacity of the system through charging and discharging during a specific running time, so as to improve the load regulation flexibility of the system. That is, the energy storage system only makes up for the inadequate regulation of the regulatory power supply load within the time period. In this study, based on the independent operation of coal-fired power, LIPBESS supplemented the load adjustment rate of the wind-coal integrated energy system to the maximum stable adjustment rate of coal-fired power. This measure can reduce the charge-discharge ratio of the energy storage system during operation and increase the operating life of the energy storage system. LIPBESS in charge and discharge function and constraints are as follows:

Charging power function of LIPBESS:

$$(P_{\text{char}})_{tj} = \frac{1}{\eta_{\text{BESS}}} \int_{1}^{(t-1)} (P_{\text{char}})_{tj} - P_{\text{r,max}} + \Delta P_{tj} \mathrm{d}t \tag{8}$$

Discharge power function of LIPBESS:

$$(P_{\text{dischar}})_{tj} = \frac{1}{\eta_{\text{BESS}}} \int_{1}^{t-1} (P_{\text{dischar}})_{tj} - P_{\text{r,max}} - \Delta P_{tj} \mathrm{d}t \tag{9}$$

$$(P_{\text{char}})_{ij} \leq P_{\text{char,max}} \tag{10}$$

$$(P_{\text{dischar}})_{ij} \leq P_{\text{dischar,max}} \tag{11}$$

P_{char} is the real-time charging power of LIPBESS; P_{dischhar} is the real-time discharge power of LIPBESS; $P_{\text{r,max}}$ is the maximum stable climbing rate of coal power; ΔP is the power adjustment value of the coal-fired power at the previous time. Eqs. (10) and (11) are the charge and discharge power constraints of the battery energy storage system, which will be introduced in detail in the following chapters.

2.2 LIPBESS Investment Costs

The investment cost of energy storage system is still an important factor restricting the construction of energy storage system. It is necessary to evaluate the construction of energy storage system by economic parameters, the economic evaluation method reference literature and local manufacturers research obtained [28,29]. The calculation method is as follows:

$$C_{\text{invest}} = C_{\text{bu}} + C_{\text{ca}} + C_{\text{ci}} + C_{\text{pc}} \tag{12}$$

$$C_{\text{bu}} = (c_{\text{b}} + c_{\text{bms}} + c_{\text{s}}) \cdot C_{\text{B}} \tag{13}$$

$$C_{\text{ca}} = (c_{\text{dc}} + c_{\text{ta}} + c_{\text{au}}) \cdot P_{\text{rated}} \tag{14}$$

$$C_{\text{ci}} = c_{\text{ci}} \cdot P_{\text{rated}} \cdot h_{\text{d}} \tag{15}$$

$$C_{\text{pc}} = c_{\text{pc}} \cdot \left(\frac{P_{\text{rated}}}{10000} \right)^{0.8} \cdot 10000 \tag{16}$$

where, C_{invest} is the total investment cost of LIPPBESS; C_{bu} is the price of major equipment of the LIPBESS; C_{ca} is the system construction and assembly costs; C_{ci} is building space and installation cost; C_{pc} is the cost of preparing auxiliary materials; C_{B} is building energy storage capacity of LIPBESS; c_{b}, c_{bms} and c_{s} the unit cost of battery original, BMS and battery storage box, respectively; c_{dc}, c_{ta}, and c_{au} are unit prices of DC/AC conversion equipment, transformer assemblies and auxiliary protection systems respectively; P_{rated} is the rated power of LIPBESS; h_{d} is each the operation time (charge/discharge) of LIPBESS; c_{ci} is the building space and installation cost required by unit energy storage system construction; c_{pc} is the cost of equipment handling required for construction.

2.3 Load Evaluation Criteria of the Power System

AGC is an important technical to guarantee the reliability operation of the grid, maintain the power generation stability of the power system and meet the needs of power users. In order to ensure the reliability of the grid, the power plant response to the AGC signal needs to satisfy certain standards.

Referring to the previous literature [30–32], three parameters are used to evaluate the AGC response of the system.

The adjustment time is an important index to evaluate whether a single load adjustment time is sufficient, and requires the difference between the instruction value and the system load to cross zero within the time period. According to the target system and the first and second frequency modulation mechanism, the single response time should last at least 30 s and the instruction period with insufficient frequency modulation time should be incorporated into the previous load evaluation, so as to filter the power grid instructions that lead to frequent unit regulation and stabilize the unit regulation frequency.

$$\begin{cases} t_{tot} = t_{ej} - t_{bj} \\ \left(\mathrm{P}_{\mathrm{system}}^{\mathrm{AGC}}\right)_{ij} - \left(\mathrm{P}_{\mathrm{system}}\right)_{ij} = 0, \quad b \le i \le e \end{cases} \tag{17}$$

where, t_{tot} is the duration of each power grid instruction; t_{bj} is the beginning moment of an instruction of the day; t_{ej} is the end time moment of an instruction of the day; $\mathrm{P}_{\mathrm{system}}^{\mathrm{AGC}}$ is the AGC instruction of a power generation system; P_{system} is the load of a power generation system.

In order to reduce the impact of the unstable stage of the adjustment rate on the evaluation results in the process of load regulation, it is necessary to obtain an effective evaluation interval in the process of load response to avoid this situation. According to the actual operation data, the evaluation interval of the average adjustment speed is 10%–90% of the process of single load adjustment, and the load adjustment speed is evaluated within this interval. The formula is as follows:

$$R_{\mathrm{AVR}} = \left(P_{hj} - P_{lj}\right) / \left(t_{hj} - t_{lj}\right) \tag{18}$$

where, R_{AVR} is the average adjustment rate of load regulation of a unit on that day; P_{hj} is the load value of each load adjustment up to 90% of the change value; P_{lj} each load adjustment up to 10% variation of the load value. Since the maximum ramp rate constrained by the model is 1.83% P_{e}/min, the standard should be lowered in the overall evaluation, and the average ramp rate evaluation index should be set to 80% (1.5% P_{e}/min) of the maximum value.

After power regulation, it is necessary to maintain the stability of power output, which requires the load fluctuation of the unit after load regulation to be within a certain range within a specified time. The load deviation degree was used to evaluate the stability after load regulation.

$$P_{\mathrm{D}} = \left[\sum_{h,j}^{e,j} \left[P_{ij} - P_{\mathrm{AGC}}\right]\right] \Big/ \left(t_{ej} - t_{hj}\right) \tag{19}$$

where, P_{D} is the degree of load deviation adjusted at the appropriate time; P_{ij} is the acual power output of power generation system. P_{AGC} is the grid instruction value of this load regulation; t_{ej} is the end time of this power grid instruction; For coal-fired power, the power fluctuation after load response adjustment stability deviation should not exceed 1% of the rated capacity.

When three evaluation parameters are met simultaneously in a load evaluation process, the adjustment process is regarded as qualified. The qualified rate of daily load evaluation is the ratio of the times of passing assessment and the total times of assessment on that day. The mathematical description is as follows:

$$(Time)_j = evaluate\left[R_{AVR}, P_D, T\right]_j \tag{20}$$

$$(A_R)_j = (Time)_j / (Time_{total})_j \tag{21}$$

where, $(Time)_j$ is the number of qualified daily load evaluation; $(A_R)_j$ is the qualified rate of daily load evaluation; $(Time_{\text{total}})_j$ Indicates the total number of daily load adjustment times.

2.4 Solution Method for Model

The model solving flow chart is shown in Fig. 2. The model is established and solved based on actual data. In this section, the coal-fired power load regulation model is solved first. The solution of wind-coal-storage integrated energy system will be introduced in Section 4.

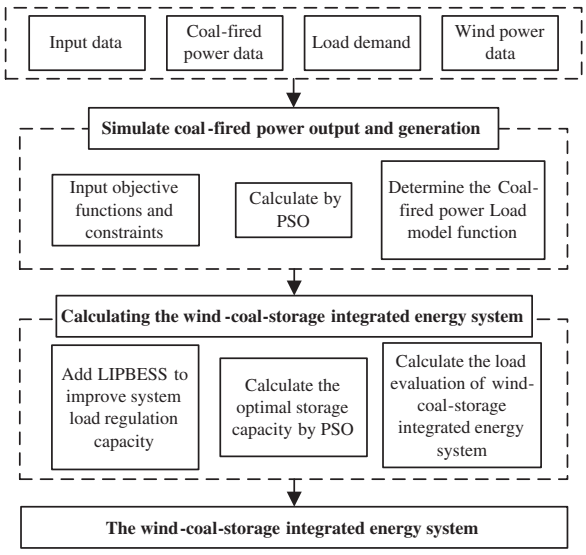

Figure 2: Model construction flow chart

The integrated energy system model and energy storage model need to be solved through actual data, which involves multi-parameter optimization. The mathematical description of the PSO solution model and objective function is as follows:

$$Object_{\text{coal}} = \min\left[\sum_{1j}^{ij}\left|(P_{real})_{ij} - (P_{\text{C}})_{ij}\right|\right] \Big/ \sum_{1j}^{ij}(P_{real}) \tag{22}$$

$$Object_{\text{BESS}} = \begin{cases} \max\left[\sum (A_R)_j/j\right] \\ \min\left(\text{B}_{\text{LIPBESS}}\right) \end{cases} \tag{23}$$

$$k_n(t) = k_n(t-1) + v_n(t-1) \tag{24}$$

$$v_n(t) = v_n(t-1) + c_n r_n\left(k_{\text{gb}}(t-1) - k_n(t-1)\right) + c_n r_n\left(k_{\text{pb}}(t-1) - k_i(t-1)\right) \tag{25}$$

$$f_{\max} = \max\left[(P_{real})_{ij} - (P_{\text{C}})_{ij}/(P_{real})_{ij}\right] \tag{26}$$

$$v_{\text{r,max}} = \frac{1}{30}\max\left|(P_{real})_{ij} - (P_{\text{C}})_{(i-30)j}\right| \tag{27}$$

where, $Object_{coal}$ is the objective function to solve the coal-fired power load model. $Object_{BESS}$ is the objective function for solving the energy storage capacity. P_{real} is the actual data of coal-fired power; A_R is the qualified rate of load evaluation; k_n $(n = 1,2,3)$ are the deviation coefficient, integral coefficient

and error coefficient respectively; v_n is the iteration speed, and the value range is [0, 0.025]; k_{pb} is called the local optimal solution, that is, the optimal solution of the single iteration interval; k_{gb} is the optimal solution for global computation; c_n is learning factors, and the value range is [0.7, 0.8]; r_n is the random weight of each iteration set to [0,1].

Since PSO may fall into the problem of local solution instead of optimal solution, this study adopts the method of generating random population iteratively at each step and enhancing the role of learning factors to avoid falling into local optimal solution. The solution process of PSO algorithm is shown in Fig. 3. P_e is the rated capacity of coal-fired power. The coal-fired power regulation model fits the typical daily actual data of each month. Different particle numbers and iteration results were calculated, as shown in Table 2.

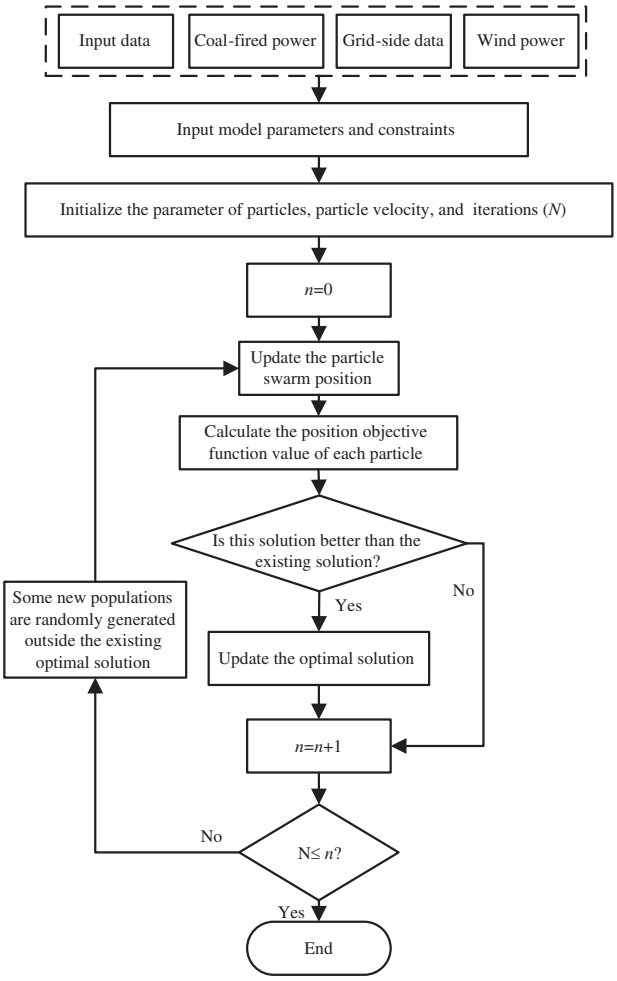

Figure 3: Flow chart of PSO algorithm solution

Table 2: Particle swarm optimization parameters and calculation results

Particle quantity	Iteration times	k_1	k_2	k_3	f (%)	f_{max} (%)	$v_{r,max}$ (P_e/min)
30	30	0.3107	0.2771	0.2845	0.3887	4.263	1.828%
50	30	0.3156	0.2219	0.2960	0.3882	4.263	1.847%
80	50	0.2722	0.4494	0.3448	0.3878	4.255	1.849%
80	100	0.2696	0.0889	0.2774	0.3876	4.257	1.857%
100	100	0.1208	0.2050	0.2772	0.3869	4.255	1.862%
150	100	0.1109	0.2723	0.2665	0.3878	4.252	1.851%
150	150	0.1106	0.2763	0.2536	0.3809	4.222	1.834%

The last group of data with the smallest error is selected as the model parameters. Therefore, it is considered that the maximum stable ramp rate of the actual data is 1.83% P_e/min, which is regarded as the constraint condition in the coal-fired power model. Verify with other daily data to ensure the maximum error is less than 5% and ensure the effectiveness of the model. The solution of energy storage configuration of wind-coal-storage integrated energy system would be introduced in the following chapters.

3 Characteristics of the Wind-Coal Integrated Energy System

3.1 Load Evaluation of the Wind-Coal Integrated Energy System

Due to the maturity of coal-fired power grid-connection technology, the load evaluation in this study takes the evaluation results of coal-power independent operation as the grid-side standard to analyze the integrated energy system. Based on the simulation results, the system load regulation process was evaluated according to the load evaluation standards, and the results were shown in Fig. 4. Compared with the independent operation of coal-fired power, the qualified rate of load evaluation of wind-coal combined power supply showed a downward trend in each month, and the decreased level was significant from January to May, and the qualified rate of average monthly load evaluation decreased by 17.1%. Compared with the load evaluation of the other five months, the independent operation level of coal-fired power in June was at a lower level. Meanwhile, the qualified rate of the load evaluation of the combined wind-coal power supply decreased the least in the six months, with an average decrease of 6.9%. In the process of these unqualified responses, the requirements cannot be satisfied in the specified period due to the insufficient variable ramp rate, which would affect the evaluation of adjacent segments. In order to further analyze the reasons for the decrease of the load evaluation qualified rate of the wind-coal combined operation, the scenarios of load regulation are analyzed in the following section.

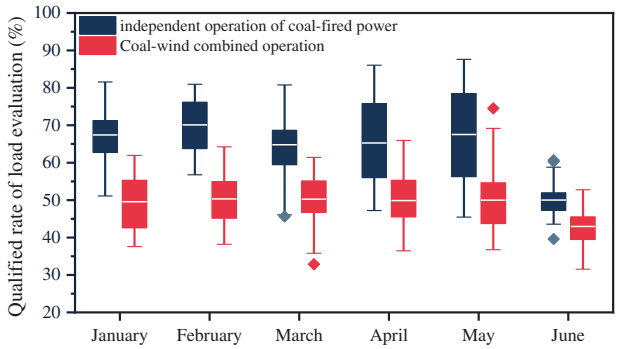

Figure 4: Load evaluation qualified rate of coal-fired power independent operation and wind-coal combined operation

3.2 Four AGC Scenarios of Wind-Coal Integrated Energy System

Wind power has volatility and randomness due to its natural characteristics. If wind power fails to respond in time to some AGC instructions during integrated energy system, it will increase the regulatory burden of the coal-fired power, which is called the phenomenon of anti-peak regulation. The load response would be unqualified when the power exceeds the regulation capacity of the coal-fired power. In the process of analyzing the data, we found that the influences for integrated energy system are distinctive for different step signal coupling. According to the different characteristics of different forms, it is divided into four scenarios. Representative data segments are selected for the explanation.

Scenario 1 as Fig. 5a: The AGC instruction of wind power decreases when the AGC instruction of the coal-fired power plant increases.

Scenario 2 as Fig. 5b: The AGC instruction of wind power increases when the AGC instruction of the coal-fired power plant decreases.

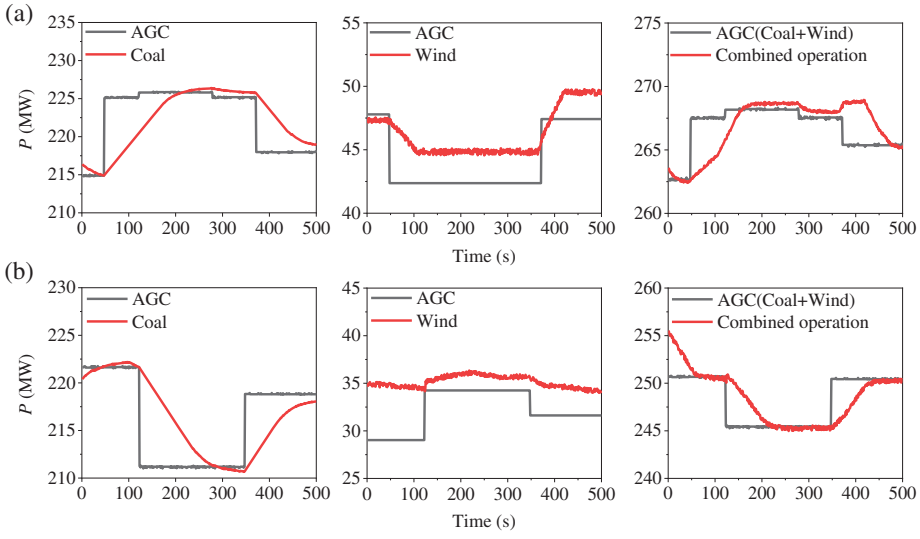

Figure 5: Schematic diagram of load response in scenario 1 and scenario 2

Compared with the original AGC instruction, the above two scenarios will reduce the target load change value which is beneficial for coal-fired power regulation. The integrated energy system in Fig. 3b reached the target load 40 s earlier. Meanwhile, these two scenarios could reduce the regulating task of the coal-fired power when the wind power can follow the target load in time, which is conducive to operation.

Scenario 3 as Fig. 6a: Wind power and coal-fired power AGC instructions elevate in synergy.

Scenario 4 as Fig. 6b: Wind power and coal-fired power AGC instructions reduce in synergy.

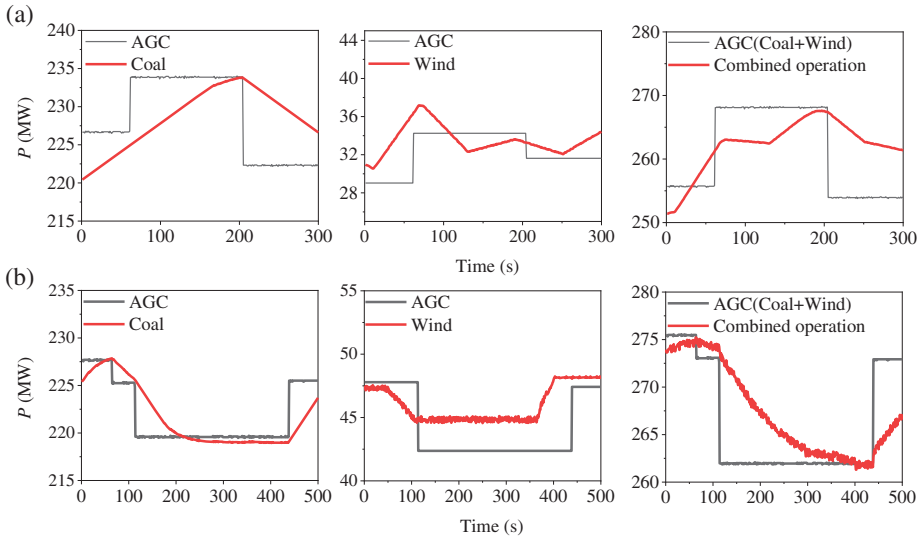

Figure 6: Schematic diagram of load response in scenario 3 and scenario 4

The above two scenarios will increase the load variation value of a single regulation for wind-coal operation, and the coal-fired power needs to operate at the maximum load regulation rate. If the wind power appears anti-peak regulating phenomenon in this period, it would increase the time required for the wind-coal system to reach the target load. Even unable to adjust the load to the instruction value within the specified time, resulting in the load adjustment failed to meet the standard, thus reducing the qualified rate of load evaluation.

3.3 Statistics of Four Scenarios under the Wind-Coal Integrated Energy System

Fig. 7 shows the average occurrence probability of various scenarios in 6 months. The results show that the proportion of each scenario changes stably in each month, and the range of change is less than 8%. On the basis of statistical results, the results are divided into two parts: regulatable and difficult to regulate, as shown in Fig. 6. Regulatable means that the load adjustment capacity of coal-fired power can adjust the load to the instruction value before the end of a certain AGC instruction, and at the same time reach the load evaluation standard. Difficult to regulate, that is, wind power appears anti-peak regulating phenomenon under the side instruction of a certain section of the grid. The probability that scenario 1 and scenario 2 are difficult to regulate is 3.5% and 4.8%, and the conditional probability is 30.2% and 22.3%, respectively. The scenario 1 and scenario 2 has little influence to the regulation of wind-coal system. In scenario 3 and scenario 4, the average proportion of system load that is difficult to regulate is 12.6% and 13.3%, respectively, and the conditional probability is 92.6% and 87.5%,

respectively. That means when scenario 3 and scenario 4 occur, it is difficult for the coal-fired power to regulate the load to reach the target load.

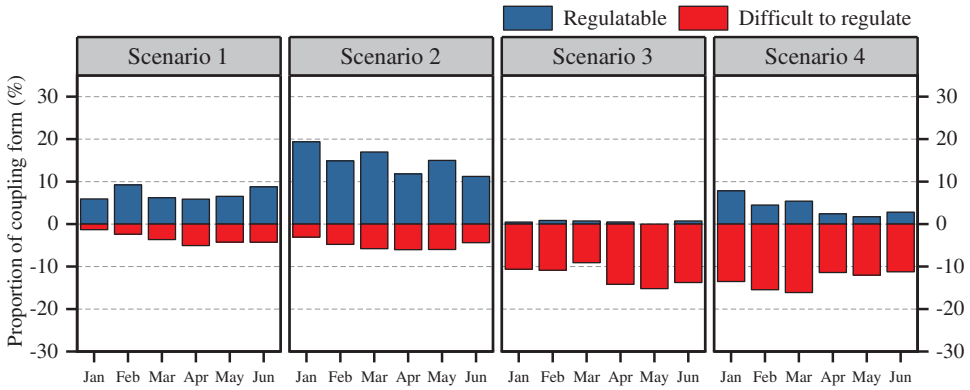

Figure 7: Statistical results of different scenarios in each month

4 The Principle of the Wind-Coal-Storage Integrated Energy System

In order to solve the problem of insufficient load regulation capacity of wind-coal system, LIPBESS was added to assist in load regulation of the system. The integrated energy system mode of the wind-coal-storage is shown in Fig. 8. The LIPBESS could enhance the flexibility of the stability of power generation by wind-coal integrated energy system through charge/discharge, alleviates power fluctuations, and promote the stable operation of wind power. Based on the four scenarios statistics of the wind-coal integrated energy system at different times, the operation strategy for LIPBESS is formulated.

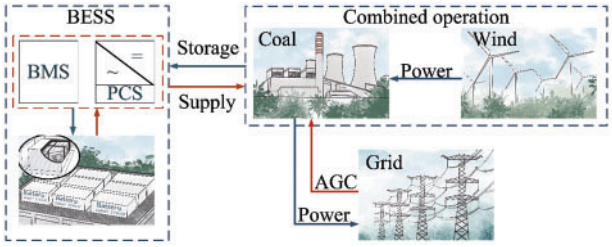

Figure 8: Diagram of wind-coal-storage combined power generation

4.1 Operation Strategies of LIPBESS

4.1.1 Typical Four Periods of the Day

According to the restriction of cycle life, it is uneconomical to charge/discharge BESS in seconds. At present, some BESS projects are in the demonstration phase. The minimum time for charging or discharging BESS is two hours [33]. Thus, the energy storage system has a very limited frequency of action in a day. Hence, we choose a relatively conservative two-charge and two-discharge models for investigation. So that the energy storage system will have a wider operation space in practical application. Meanwhile, to ensure the LIPBESS could fully charge and discharge at least 50% of the time in each period, the maximum charge/discharge power per MWh in LIPBESS is limited to 0.5 MW.

The day is divided into four periods to formulate the LIPBESS operation strategy. From the perspective of daily activities. 0:00–6:00 at night, with fewer personnel activities and less corresponding power demand. Therefore, it is considered that the load demand changes less during this period compared with other times. 6:00–12:00, personnel activities gradually increase, most industries began to operate, and electricity demand gradually increases during this period. 12:00–18:00, actual coal-fired plants are usually at higher load levels during this period. 18:00–24:00, personnel activities and power demand gradually decrease until relatively stable low-level load demand. According to the five scenarios instruction for wind-coal in different periods, the proportion of difficult to regulate the load in each scenario in the wind-coal integrated energy system in each period was calculated.

4.1.2 The Charge/Discharge Period of the LIPBESS

According to scenario division, the priority degree of charge and discharge taken by LIPBESS in different scenario s is determined. When anti-peak regulating occurs in scenario 3, LIPBESS discharge is needed to improve the system load within the period to meet the demands of the grid-side. Similarly, scenario 4 requires LIPBESS charging to reduce the system load during the time period. According to the analysis in the previous section, the occurrence probability of scenario 1 and scenario 2 is low. Meantime, when the load in scenario 1 and scenario 2 is difficult to adjust, the requirements for charging and discharging are similar to those in scenario 3 and Scenario 4, which are suitable for discharging and charging respectively. Therefore, the LIPBESS preferentially charges/discharges according to the probability of difficulty adjustment in scenario 3 and scenario 4.

According to the division of time periods, the probability of scenario 3 and scenario 4 is calculated in different time periods. The boxplot of statistical results for each time period is shown in Fig. 9. Based on the statistical results, the operation of energy storage is divided into two quarters, January to March and April to June. In the first quarter, the average probability of scenario 4 occurring at 0:00–6:00 h and 12:00–18:00 h was 5.2% and 3.8% higher than that of scenario 3, and LIPBESS was preferably charged. The ratio between 6:00–12:00 and 18:00–24:00 in scenario 3 is higher than that in scenario 4, which is 7.7% and 6.2% higher on average. Therefore, the LIPBESS gives priority to discharge operation.

In the second quarter, at 0:00–6:00 and 12:00–18:00, the average probability of difficulty adjustment in scenario 3 is 9.2% and 3.6% higher than that in scenario 4, and the LIPBESS gives priority to discharge. The occurrence probability of scenario 4 at 6:00–12:00 and 18:00–24:00 is 6.3% and 4.7% higher than that of scenario 3 on average, so the charging operation is preferred.

In summary, the operation strategy of the LIPBESS in the integrated energy system is as follows: the operation mode of charge-discharge-charge-discharge is carried out in the first quarter, and the operation mode of discharge-charge-discharge-charge is adopted in the second quarter.

4.2 The Optimal Storage Capacity of LIPBESS

In order to plan the optimal LIPBESS configuration, the influence of different energy storage system capacities on the monthly average operation qualified rate is preliminarily explored, as shown in Fig. 10. The results show that the LIPBESS enhances the qualified rate of the wind-coal integrated energy system, and the qualified rate increases with the increase of energy storage capacity. However, due to the fixed operation mode of energy storage in the day, the qualified rate of the wind-coal-storage system has a limit in theory. It can be seen from Fig. 10 that compared with 5 MWh, the qualified rate of 6 MWh is only improved by 3.2% on average. Therefore, there is an optimal scenario for the wind-coal-storage integrated energy system.

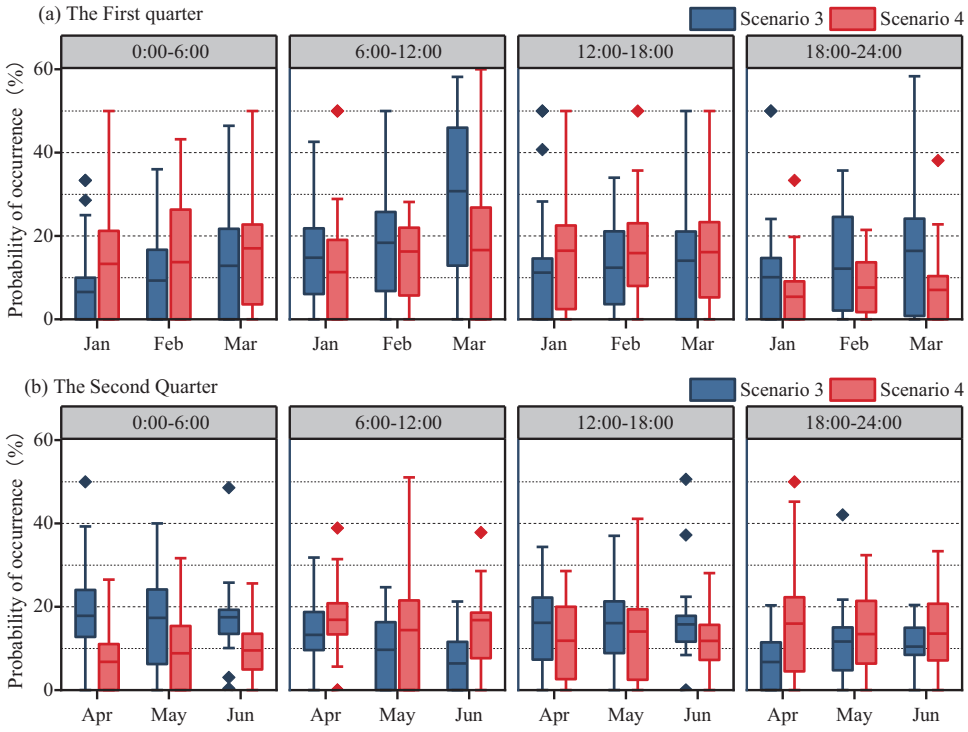

Figure 9: Probability statistics of scenario 3 and scenario 4 in each period

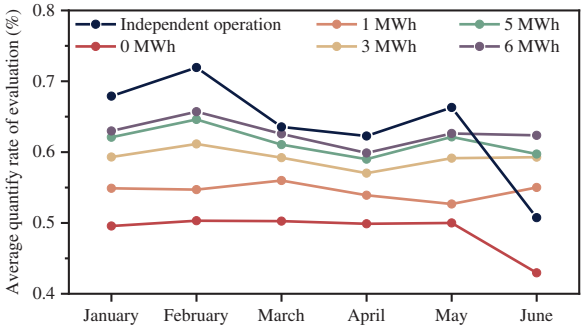

Figure 10: The qualified rate of combined operation under each BESS capacity

On this basis, the energy storage capacity is optimized by taking the average load evaluation qualified rate and minimizing construction cost as the objection. PSO is adopted in which the two objective functions are the maximum average load and the minimum LIPBESS capacity. The optimal LIPBESS capacity is 5.5 MWh through the calculation of the wind-coal-storage integrated energy system model.

4.3 Power Generation Evaluation of Wind-Coal-Storage Integrated Energy System

The LIPBESS adopts two charge/discharge operation modes through scenario analysis. The energy storage only charges or discharges in a certain period to improve the ramp rate of the system, without other adjustments. Fig. 11 shows the qualified rate of wind-coal-storage evaluation. The

particular reason for the higher qualified rate is that the addition of LIPBESS enhances the ramp rate of the combined power generation. Compared with the wind-coal combined power generation system without LIPBESS, the qualified rate of wind-coal-storage integrated energy system is increased by 14.5% per month. The biggest increase was in June, at 15.7%. The average qualified rate of wind-coal-storage integrated energy system in March and June reached the level of independent operation of coal-fired power, and the average difference between the system and independent operation of coal-fired power in other months was only 5.4%. The integrated energy system of the wind-coal-storage in this paper consists of a 50 MW wind farm combined with a 5.5 MW LIPBESS and a 330 MW coal-fired power. Using the wind-storage operation method in reference [34], at least 12 MWh BESS capacity is required to adapt to a 50 MW wind farm to make wind power have better scheduling. In addition, the wind-coal-storage integrated energy system mode fully uses the existing regulation potential of the coal-fired power to enhance the utilization of the wind power generation, and LIPBESS shares the task of power regulation in the process. Compared with the wind-storage operation, the capacity demand for energy storage is reducing. The economic indicators of LIPBESS were obtained from manufacturer and reference [28,29], as shown in Table 3. The construction cost of the energy storage system required by the coal integrated energy system is $1,334,031.9, saving $15,48,323.1 compared to the investment of the wind-storage integrated energy system (12 MWh) with the same calculation parameters.

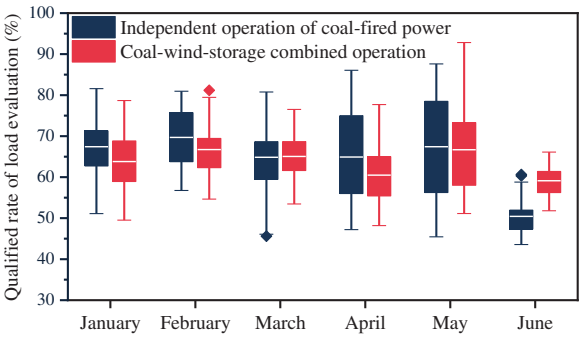

Figure 11: The qualified rate of wind-coal-storage integrated energy system

Table 3: LIPBESS investment cost parameters

Parameter	Value	Unit
Battery pack price (c_b)	157.2	$/kWh
BMS (c_{bms})	31.44	$/kWh
Battery storage box (c_s)	18.86	$/kWh
DC/AC conversion equipment (c_{dc})	25.93	$/kWh
Transformer (c_{ta})	0.94	$/kWh
Auxiliary protection system (c_{au})	31.44	$/kWh
Building space and installation cost (c_{ci})	1.57	$/kWh
Preliminary engineering preparation (c_{pc})	4.41	$/kWh
Major equipment (C_{bu})	1,141,250	$
Construction and assembly cost (C_{ca})	160,352.5	$
Building space and installation cost (C_{ci})	17,270	$

(Continued)

Table 3 (continued)

Parameter	Value	Unit
Preparing auxiliary materials (C_{pc})	15,159.4	$
Investment cost, wind-coal-storage (C_{invest})	1,334,031.9	$
Investment cost, wind-storage (C_{invest})	2,882,355.0	$

Based on the above results, the advantages of extensive distribution, large installed capacity, and the flexibility of existing coal-fired power plants should be fully utilized during the process of gradually reducing coal-fired power generation. Different plants can operate combined with dissimilarly wind power capacities. The analysis results of the wind-coal-storage integrated energy system explored in this paper show that coal-fired power plants can dispatch wind power, but there are certain limitations to this ability. The 330 MW coal-fired power can dispatch 50 MW wind power generation by adding a 5.5 MWh energy storage system. At the same time, coal-fired plants have huge installed capacity worldwide and have great potential in dispatching renewable energy, and the price of lithium-ion batteries is gradually reduced. In real terms, the load regulation potential of coal-fired power is not only limited by 1.83 P_e%/min calculated in this paper, which means that there is room for further research on the absorption of wind power by coal-fired power plants.

5 Conclusions

This paper discusses the feasibility of using the flexible advantages of coal-fired power and LIPBESS to dispatch wind power. Through the statistics and analysis of the four scenarios, the energy storage operation strategy of two charge/discharge is formulated. Taking the actual user load demand and the optimal LIPBESS construction as the objection, the wind-coal-storage system is established under the actual data of the power plant. The results show that:

1. The anti-peak regulating phenomenon is the main reason that increases the difficulty of wind-coal system load regulation in scenario 3 and scenario 4. The simulation results show that the qualified rate of the wind-coal integrated energy system decreases significantly from January to May, and the qualified rate of the average daily load evaluation decreases by 17.1%, which is difficult to meet the requirements of grid-side stability.

2. Lithium-iron phosphate battery energy storage system (LIPBESS) was added to adjust the load of the system, and the operation mode of wind-coal-storage integrated energy system was constructed. According to the occurrence probability of different time periods, different scenarios and the priority of energy storage charging/discharging and the LIPBESS operation strategy of two-charge and two-discharge was developed. By PSO optimization calculation, the optimal LIPBESS capacity of wind-coal-storage integrated energy system is 5.5 MWh.

3. In March and June, the average qualified rate of wind-coal-storage integrated energy system reached the level of independent operation of coal-fired power. In other months, the average difference was only 5.4%, which show that the wind-coal-storage integrated energy system could meet the demand of grid-side stability. Compared with the wind-storage mode, the energy storage capacity and investment cost are reduced by 54.2% and 53.7%, respectively.

Acknowledgement: Thanks for the support of the North China Electric Power University, Natural Science Foundation of China, Natural Science Foundation of Hebei Province and the Fundamental Research Funds for the Central Universities.

Funding Statement: The study was supported by the Natural Science Foundation of China (Grant No. 52076079), Natural Science Foundation of Hebei Province, China (Grant No. E2020502013), the Fundamental Research Funds for the Central Universities (2021MS076, 2021MS079).

Conflicts of Interest: The authors declare that they have no conflicts of interest to report regarding the present study.

References

1. Shu, H., Jiang, X., Cao, P., An, N., Tian, X. et al. (2020). Time-domain protection for transmission lines connected to wind power plant based on model matching and hausdorff distance. *Energy Engineering, 118(1),* 53–71. https://doi.org/10.32604/EE.2020.012381
2. Zhang, M., Li, H., Deng, X. (2021). Inferential statistics and machine learning models for short-term wind power forecasting. *Energy Engineering, 119(1),* 237–252. https://doi.org/10.32604/EE.2022.017916
3. Zhang, N., Lu, X., McElroy, M. B., Nielsen, C. P., Chen, X. et al. (2016). Reducing curtailment of wind electricity in China by employing electric boilers for heat and pumped hydro for energy storage. *Applied Energy, 184(5946),* 987–994. https://doi.org/10.1016/j.apenergy.2015.10.147
4. Chaychizadeh, F., Dehghandorost, H., Aliabadi, A., Taklifi, A. (2018). Stochastic dynamic simulation of a novel hybrid thermal-compressed carbon dioxide energy storage system (T-CCES) integrated with a wind farm. *Energy Conversion and Management, 166(5),* 500–511. https://doi.org/10.1016/j.enconman.2018.04.050
5. Nassar, Y. F., Abdunnabi, M. J., Sbeta, M. N., Hafez, A. A., Amer, K. A. et al. (2021). Dynamic analysis and sizing optimization of a pumped hydroelectric storage-integrated hybrid PV/wind system: A case study. *Energy Conversion and Management, 229(1),* 113744. https://doi.org/10.1016/j.enconman.2020.113744
6. Zhang, Z., Ding, T., Zhou, Q., Sun, Y., Qu, M. et al. (2021). A review of technologies and applications on versatile energy storage systems. *Renewable and Sustainable Energy Reviews, 148(3),* 111263. https://doi.org/10.1016/j.rser.2021.111263
7. Rehman, S., Salman, U., Alhems, L. (2020). Wind farm-battery energy storage assessment in grid-connected microgrids. *Energy Engineering, 117(6),* 343–365. https://doi.org/10.32604/EE.2020.011471
8. Hannan, M. A., Wali, S. B., Ker, P. J., Rahman, M. S. A., Mansor, M. et al. (2021). Battery energy-storage system: A review of technologies, optimization objectives, constraints, approaches, and outstanding issues. *Journal of Energy Storage, 42,* 103023. https://doi.org/10.1016/j.est.2021.103023
9. Zeng, M., Cao, H., Pan, T., Hu, P., Tian, S. et al. (2022). Typical application scenarios and economic benefit evaluation methods of battery energy storage system. *Energy Engineering, 119(4),* 1569–1586. https://doi.org/10.32604/ee.2022.019488
10. Lu, L., Yuan, W., Su, C., Wang, P., Cheng, C. et al. (2021). Optimization model for the short-term joint operation of a grid-connected wind-photovoltaic-hydro hybrid energy system with cascade hydropower plants. *Energy Conversion and Management, 236(3),* 114055. https://doi.org/10.1016/j.enconman.2021.114055
11. Yoshiba, F., Hanai, Y., Watanabe, I., Shirai, H. (2021). Methodology to evaluate contribution of thermal power plant flexibility to power system stability when increasing share of renewable energies: Classification and additional fuel cost of flexible operation. *Fuel, 292,* 120352. https://doi.org/10.1016/j.fuel.2021.120352
12. Kopiske, J., Spieker, S., Tsatsaronis, G. (2017). Value of power plant flexibility in power systems with high shares of variable renewables: A scenario outlook for Germany 2035. *Energy, 137(1),* 823–833. https://doi.org/10.1016/j.energy.2017.04.138

13. Garðarsdóttir, S. Ó., Göransson, L., Normann, F., Johnsson, F. (2018). Improving the flexibility of coal-fired power generators: Impact on the composition of a cost-optimal electricity system. *Applied Energy, 209,* 277–289. https://doi.org/10.1016/j.apenergy.2017.10.085
14. Zhu, M., Wu, X., Shen, J., Lee, K. (2021). Dynamic modeling, validation and analysis of direct air-cooling condenser with integration to the coal-fired power plant for flexible operation. *Energy Conversion and Management, 245,* 114601. https://doi.org/10.1016/j.enconman.2021.114601
15. Frew, B. A., Becker, S., Dvorak, M. J., Andresen, G. B., Jacobson, M. Z. (2016). Flexibility mechanisms and pathways to a highly renewable US electricity future. *Energy, 101,* 65–78. https://doi.org/10.1016/j.energy.2016.01.079
16. Ye, L. C., Lin, H. X., Tukker, A. (2019). Future scenarios of variable renewable energies and flexibility requirements for thermal power plants in China. *Energy, 167,* 708–714. https://doi.org/10.1016/j.energy.2018.10.174
17. Li, L. Y., Dai, M., Hao, S., Qiu, G., Li, G. et al. (2021). Optimal generation expansion planning model of a combined thermal-wind–PV power system considering multiple boundary conditions: A case study in Xinjiang. *China Energy Reports, 7(6),* 515–522. https://doi.org/10.1016/j.egyr.2021.01.020
18. Gao, X., Liu, W., Fu, M., Zhang, S., Zhang, S. et al. (2021). Strategy decision game approach of the combination generation system of wind and thermal power participating in the direct power purchase transaction of large consumer. *Electric Power Systems Research, 200(12),* 107463. https://doi.org/10.1016/j.epsr.2021.107463
19. Dong, Y., Jiang, X., Ren, M., Yuan, J. (2019). Environmental implications of China's wind-coal combined power generation system. *Resources, Conservation and Recycling, 142(1),* 24–33. https://doi.org/10.1016/j.resconrec.2018.11.012
20. Zhu, Y., Wang, J., Qu, B. (2014). Multi-objective economic emission dispatch considering wind power using evolutionary algorithm based on decomposition. *International Journal of Electrical Power & Energy Systems, 63(1),* 434–445. https://doi.org/10.1016/j.ijepes.2014.06.027
21. Dong, J., Han, S., Shao, X., Tang, L., Chen, R. et al. (2021). Day-ahead wind-thermal unit commitment considering historical virtual wind power data. *Energy, 235(6),* 121324. https://doi.org/10.1016/j.energy.2021.121324
22. Zhang, N., Lu, X., McElroy, M. B., Nielsen, C. P., Chen, X. et al. (2016). Reducing curtailment of wind electricity in China by employing electric boilers for heat and pumped hydro for energy storage. *Applied Energy, 184(5946),* 987–994. https://doi.org/10.1016/j.apenergy.2015.10.147
23. Wang, G., Zhang, L., Ai, D., Zhao, Y., Zhou, Y. (2020). Research on Nox formation and SCR denitration system control by smoke mixing under low load. *2019 5th International Conference on Environmental Science and Material Application*, 042053. Bristol, Iop Publishing Ltd.
24. Zhao, E., Gu, Y., Fang, S., Yang, L., Hirano, S. (2021). Systematic investigation of electrochemical performances for lithium-ion batteries with Si/Graphite anodes: Effect of electrolytes based on fluoroethylene carbonate and linear carbonates. *ACS Applied Energy Materials, 4(3),* 2419–2429. https://doi.org/10.1021/acsaem.0c02946
25. Tang, H., Wu, Y., Cai, Y., Wang, F., Lin, Z. et al. (2022). Design of power lithium battery management system based on digital twin. *Journal of Energy Storage, 47,* 103679. https://doi.org/10.1016/j.est.2021.103679
26. Wang, Y., Sun, Y., Zhang, Y., Chen, X., Shen, H. et al. (2022). Optimal modeling and analysis of microgrid lithium iron phosphate battery energy storage system under different power supply states. *Journal of Power Sources, 521(4),* 230931. https://doi.org/10.1016/j.jpowsour.2021.230931
27. Wang, Y., Pan, R., Liu, C., Chen, Z., Ling, Q. (2018). Power capability evaluation for lithium iron phosphate batteries based on multi-parameter constraints estimation. *Journal of Power Sources, 374(2),* 12–23. https://doi.org/10.1016/j.jpowsour.2017.11.019

28. Chen, X., Huang, L., Liu, J., Song, D., Yang, S. (2022). Peak shaving benefit assessment considering the joint operation of nuclear and battery energy storage power stations: Hainan case study. *Energy, 239(11),* 121897. https://doi.org/10.1016/j.energy.2021.121897
29. Sun, B., Su, X., Wang, D., Zhang, L., Liu, Y. et al. (2020). Economic analysis of lithium-ion batteries recycled from electric vehicles for secondary use in power load peak shaving in China. *Journal of Cleaner Production, 276(1),* 123327. https://doi.org/10.1016/j.jclepro.2020.123327
30. Lobato, E., Egido, I., Rouco, L. (2012). Monitoring frequency control in the Turkish power system. *Electric Power Systems Research, 84(1),* 144–151. https://doi.org/10.1016/j.epsr.2011.10.016
31. Pandey, S. K., Mohanty, S. R., Kishor, N. (2013). A literature survey on load-frequency control for conventional and distribution generation power systems. *Renewable and Sustainable Energy Reviews, 25(7),* 318–334. https://doi.org/10.1016/j.rser.2013.04.029
32. Parmar, K. P. S., Majhi, S., Kothari, D. P. (2012). Load frequency control of a realistic power system with multi-source power generation. *International Journal of Electrical Power & Energy Systems, 42(1),* 426–433. https://doi.org/10.1016/j.ijepes.2012.04.040
33. Shandong Energy Regulatory Office (2021). Shandong power auxiliary service market operating rules. http://sdb.nea.gov.cn/tzgg/content_6873
34. Teleke, S., Baran, M. E., Bhattacharya, S., Huang, A. Q. (2010). Rule-based control of battery energy storage for dispatching intermittent renewable sources. *IEEE Transactions on Sustainable Energy, 1(3),* 117–124. https://doi.org/10.1109/TSTE.2010.2061880